Unsteady transition from a Mach to a regular shockwave intersection

S. J. KARABELAS and N.C. MARKATOS
Department of Chemical Engineering, Computational Fluid Dynamics Unit
National Technical University of Athens (N.T.U.A.)
9, Heroon Polytechniou str., Zografou, GR-15780
GREECE
email:stkarabelas@hotmail.com

Abstract: The purpose of this research work is to perform accurate numerical computations of supersonic flow in a converging nozzle and specifically to study Mach-disks. The latter process has been widely studied over the last years. In the present study numerical simulations are performed for transient supersonic flow, tracing the transition from a Mach reflection to a regular one. This has been done by enforcing the walls of a converging nozzle to come closer together, changing the deflection angle with time. Viscosity was taken into account and the full Navier-Stokes have been solved. The results obtained clearly show the gradual extinction of the Mach disk and the eventual wave intersection to a single point.

Key-Words: supersonic flow, Mach disk, shock waves, Mach intersection

1 Introduction

A symmetrical parabolic converging nozzle of inlet diameter 4 m and outlet 3 m was used to generate shock waves (Fig.1). According to shock reflection theory, when the shock angle φ is smaller than the Von-Neumman critical angle φ_v the shock wave reflects into a regular reflection. In our case both shock waves induced from the top and bottom walls intersect to a regular intersection (single point) [2]. For shock angles greater than the detachment angle φ_d a Mach intersection will be induced, which means that the intersecting waves form a Mach disk [6]. In the range between φ_v and φ_d both types of reflection could be induced.

Despite the existence of those critical angles, the transition conditions are not very clear. There are differences between experimental and numerical results, especially in the Mach disk region and considerable disagreement between numerical and theoretical values concerning the above mentioned critical angles.

The waves' intersection closely to an axis of symmetry is examined here. At the inlet region, due to the deflection of walls, oblique shock waves are formed. These waves intersect at two points, known as Mach or triple points, leading to a normal shock wave, the Mach disk. Afterwards these waves reflect on the walls downstream. According to theory, depending on flow conditions, there form two slip lines or discontinuity lines and a vortex sheet.
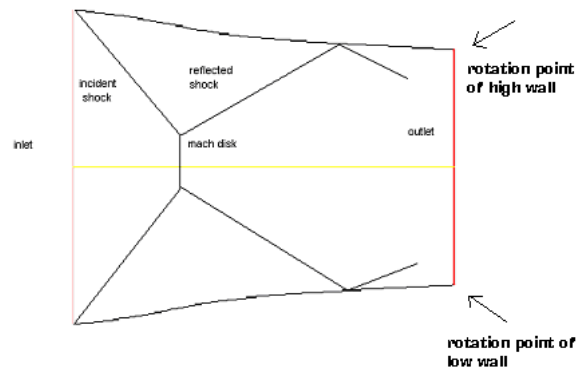

Fig. 1. Shock wave intersections, causing mach disk.

In transient problems hysterisis is observed, due to the continuous changes of the deflection angle. The result is transitions from Mach to regular reflections and vice versa. In more detail when the deflection angle is less than θ_v (Von-Neumann criterion) then we have regular reflection. When it reaches the value θ_d (the detachment angle) we get Mach reflection. Then θ decreases (deflection angle is the maximum angle), while the shock reflection remains Mach, and when it reaches again θ_v we have conversion to regular. This cyclic behaviour denotes that the phenomenon presents hysterisis. Only the transition process is dealt with in this work.

2 Solving the flow equations

2.1 The mathematical problem

The flow is described by the Navier-Stokes equations as applied for supersonic flight. The discretized equations must be set up considering the movement of the grid since the flow passes through moving boundaries (walls). For that reason the velocity vector $\underline{\upsilon}$ is equal to the difference of the absolute flow velocity and grid velocity of the moving mesh. The equations are hyperbolic in nature and in an abbreviated form are as follows [9]:

$$\frac{\partial \rho}{\partial t} + \nabla \cdot (\rho \underline{\upsilon}) = 0 \qquad (1)$$

$$\frac{\partial}{\partial t}(\rho \underline{\upsilon}) + \nabla(\rho \underline{\upsilon}\,\underline{\upsilon}) = -\nabla p + \nabla(\underline{\tau}) \qquad (2)$$

where $\underline{\tau} = \mu[(\nabla \underline{\upsilon} + \nabla \underline{\upsilon}^T) - \frac{2}{3}\nabla \underline{\upsilon} I]$ (*I* is the unit tensor)

$$\frac{\partial}{\partial t}(\rho E) + \nabla \cdot (\upsilon(\rho E + p)) = \nabla \cdot (k_{eff}\nabla T - (\underline{\tau}\,\underline{\upsilon})) \qquad (3)$$

where $E = h - \dfrac{p}{\rho} + \dfrac{\upsilon^2}{2}$

The symbols μ, ρ , $p, \underline{\upsilon}$, $\underline{\tau}$, k_{eff} , h, *T,E,* respectively, denote molecular viscosity, density, static pressure, velocity vector, stress tensor, total thermal conductivity, enthalpy, static temperature and energy.

2.2 Numerical Solution and Turbulence Modelling

The above differential equations are solved by the finite volume technique. The SIMPLE-Consistent algorithm was chosen for accounting for the pressure-velocity coupling [17]. First order upwind scheme was used for the convective terms and central for the diffusion terms. The temporal discretization was also of first order.

The formulation for this scheme was fully implicit and the system of the algebraic equations for every time step was solved iteratively by a classic Gauss-Seidel point iterative method,. For reasons of convergence acceleration, a pseudo-time step

relaxation was used in every time step with a suitable relaxation factor. Also was used a classic V-cycle multigrid algorithm for the same reason.

Turbulence modelling was used when accounting for the viscous solutions of equations. For that purpose the Spalart-Allmaras model [15] was chosen, which solves only one equation, the equation for eddy viscosity. The model was designed initially for low Reynolds numbers but it is used widely for aerospace applications (transonic-supersonic speeds) [5], despite the fact that its dependent variable is a fictitious one.

The transport equation for the eddy viscosity v is derived by arguments of dimensional analysis and Galilean invariance, and is given by:

$$\frac{\partial}{\partial t}(\rho v) + \frac{\partial}{\partial x_i}(\rho v u_i) = G_v + \frac{1}{\sigma_v}[\frac{\partial}{\partial x_j}\{(\mu + \rho v)\frac{\partial v}{\partial x_j}\} + C_{b2}\rho(\frac{\partial v}{\partial x_j})^2] - Y_v$$

(4)

$$G_{v=}C_{b1}\rho Sv\,, S = S_1 + vf_{u2} / k^2 d^2\,, f_{u2} = 1 - \frac{\chi}{\chi f_{u1}}\,,$$

$$Y_v = C_{w1}\rho f_w(\frac{v}{d})^2$$

where G_v is the production of turbulence viscosity and Y_v is the destruction of turbulence viscosity that occurs in the near-wall region. The symbols d ,S,χ f_{u2} , f_{u1} respectively, denote wall distance, deformation tensor, ratio of molecular to kinematic viscosity and functions of molecular and kinematic viscosity. The other symbols are constants

For the numerical solution of supersonic flow inside the nozzle, two commercial codes were used, FLUENT 6.1.18 2d version (solver) and GAMBIT 2.1.6. (mesh generator), both provided by Fluent Inc.

An unstructured mesh of 67000 cells was employed. Inlet conditions were: atmospheric pressure and Mach number of 1.8 and outlet conditions, pressure of 255000 pascal. No slip conditions apply at both nozzle walls and classic wall functions were used [18].

Density is computed via the perfect gas law (admission of isentropic flow). Finally, corcerning the molecular viscosity μ, because during a supersonic flow there exist substantial temperature gradients, a function was defined, which describes the changes of viscosity with respect to temperature. The law of Sutherland [5] was chosen:

$$\mu(T) = \mu_o \left(\frac{T}{T_o}\right)^{1.5} \frac{T_o + 110.56}{T + 110.56}$$

where $T_o = 273.16$ K and $\mu_o = 1.78$ kgm^{-1}s^{-1} are the reference values.

Due to the movement of the wall boundaries (as they approach each other) the mesh must be updated with time. Specifically the walls move with the rotation speed of 3 degrees per second. The original point of rotation is the edge point of outlet for every wall respectively (Fig.1). As a result it is obvious that the grid is continuously deforming and it has to be updated at every time step. The main techniques applied for updating the deforming mesh is the spring-based smoothing method and local remeshing**. The last method has been described in detail in Anthony Anderson's research work [16].

2.3. Grid refinement and time independency.

Three different unstructured meshes were generated in order to indicate which mesh is independent of further grid refinement. Fig.2 shows the pressure distribution along the axis of symmetry for the three meshes. That of 67000 cells has almost the same distribution of the most refined mesh. The same is true for the other variables as well. So it was selected for time saving reasons (cpu time).

The second step is the time independency investigation. For this purpose we considered three different time steps (0.05, 0.1 and 0.2 sec). Again pressure distributions are presented at the symmetry plane for three different time positions. Fig. 3 shows that the choice of time step 0.1 sec is acceptable.
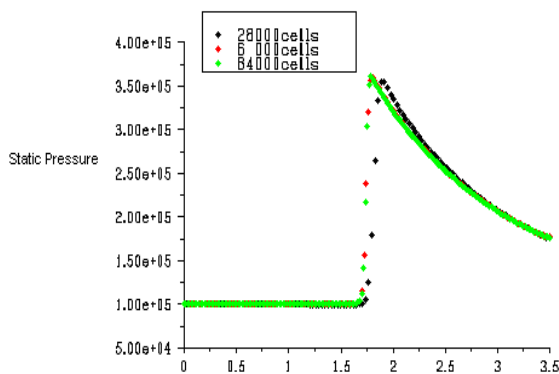
different meshes.

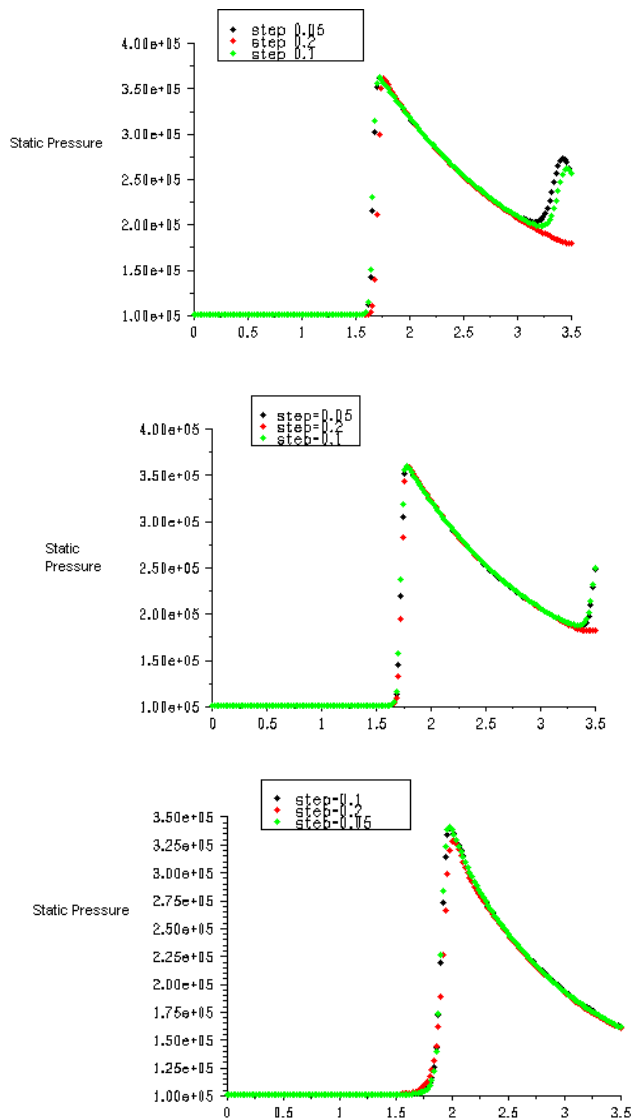
Fig.3. Pressure distribution along axis of symmetry for three different time steps: t=0.2 sec, 0.6 sec and 1.2 sec from top to bottom respectively

3 Results and discussion

Computational results were obtained on a Pentium IV Machine with a cpu time of about 6 hours for full convergence of the primitive variables: x and y velocity, eddy viscosity and static pressure. Convergence is deemed to occur when the scaled residuals fall below 10e-5. The total number of time steps was 16, from 0.1 sec to 1.6 sec.

Fig.2. Pressure distribution along axis of symmetry for three

Beginning the analysis of results, and observing at time t=0.2 sec the Mach contours, we see the Mach disk formed around the middle of the axis (Fig.4). At the next time steps, we can easily observe both walls approaching each other. As a result, the deflection angle is decreasing, causing the reduction of disk's length. After 1.5 seconds the Mach disk does no longer exist and the waves intersect at a regular intersection.
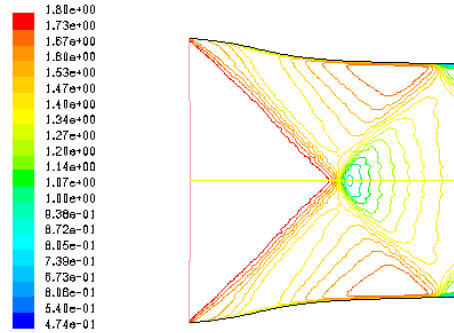
Fig. 4 illustrates the presence of an additional process. The disk is moving towards the outlet with time, and the decrease of the deflection angle causes a corresponding decrease to the shock angle of the waves. As a result they become weaker and of course they expand more in the flow domain.
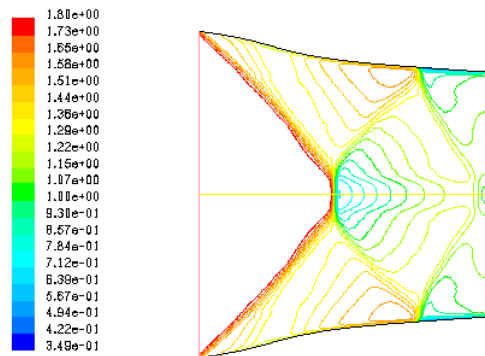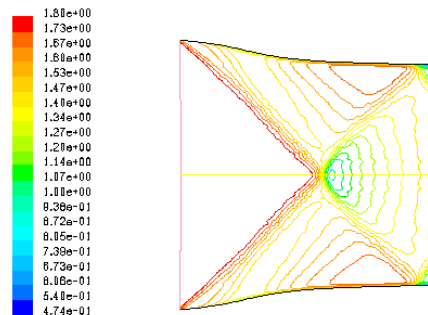

t=0.2 sec
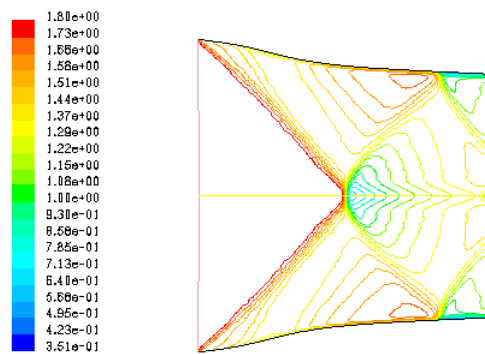
t=0.9 sec

t=1.3 sec

t=1.6 sec

Fig.4. Mach contours plotted versus time (t=0.2sec to 1.6 sec).

3.1 Transition from Mach to Regular intersection..

In shock wave reflection studies a main objective is to compute the height and position of the Mach disk versus time. In this study, the independent variable is not the wedge angle, as used in most studies, but time, because of the transient nature of the process. To perform height computation we need information at every time provided by the results obtained until then. Because the Mach disk is a normal shock wave, we trace the region where considerable discontinuities occur (subsonic to supersonic flow). This criterion gives us direct guidelines for evaluating the height value. At first place the Mach number distribution at the axis plane is estimated. Fig. 5 displays a significant decrease of Mach number, indicating the position where the Mach disk begins to expand. The first point of this spontaneous change defines the starting point of disk's thickness. The flow there

remains supersonic. Behind that point, flow becomes subsonic. In this region we make a normal section (direction parallel to the y axis), and we compute the Mach number distribution in this section. We observe that as we move towards the wall (positive y), the Mach number increases (Fig. 6). There is a point where the flow becomes sonic (*M=1*). After that point the flow returns supersonic. The sonic point indicates where the height of the Mach disk ends. This sonic point is the Mach or triple point as mentioned above. Following this process at all time positions, we estimate height as a function of time. Fig. 7 shows that height decreases with time and becomes zero (regular reflection) at time=1.5 sec.
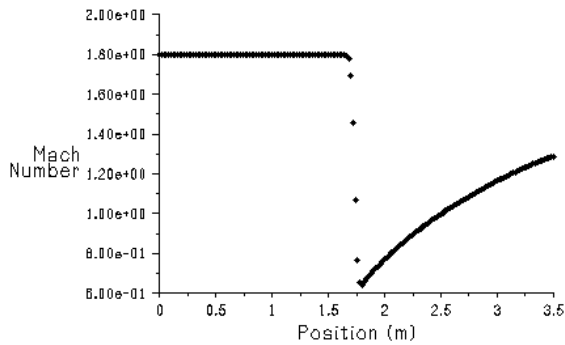
time (Fig.8). It is obvious that the disk moves towards the outlet.
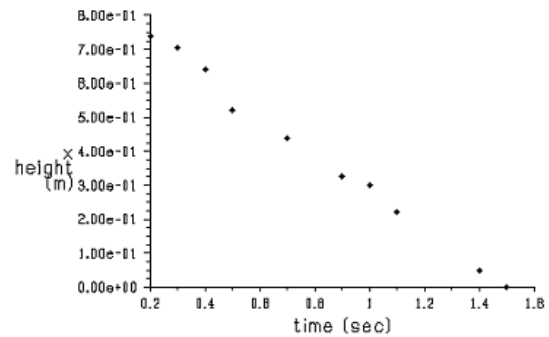
Fig. 7. Disk height varying with time.

Fig.5 Mach number distribution along the axis of symmetry plane
        at a particular time step.

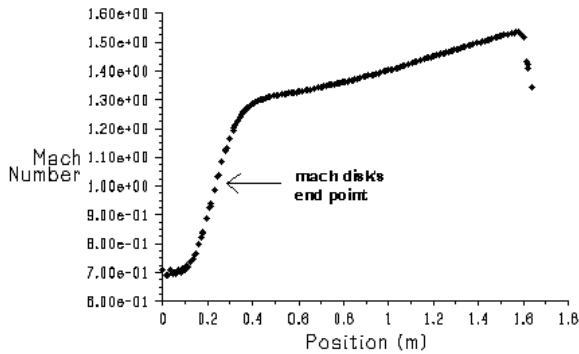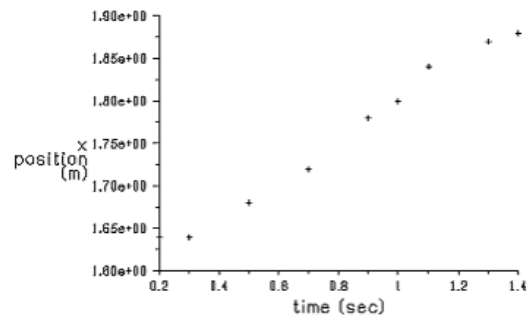Fig. 8. Disk position along axis of symmetry plotted against
        time.

Fig.6. Mach number distribution at the symmetry plane
    at x=1.77m.

Based on the above procedure, we compute the change of Mach disk's position. From Fig. 6 we find the beginning of disk's thickness. Repeating for the remaining time steps, we plot the disk position versus

4 Conclusions

Numerical simulations have been carried out, by means of special numerical and mesh-update techniques. The system equations have been solved by a segregated (not coupled) manner, using known point iterative methods. Flow viscosity was taken into consideration and the full Navier- Stokes equations were solved. The results appear plausible and the shock position and sharpness were predicted accurately without the need for special shock capturing techniques.

Finally giving a further interest for numerical research, it would be very interesting to apply periodic movement to the walls, i.e. making them converging and diverging. Then the Mach disk would periodically form and then vanish, depicting the hysterisis process.

References:
[1] J.D. Anderson, *Supersonic and High Temperature Gas Dynamics*, McGraw-Hill, 1989.
[2] Chapman CJ. *High Speed Flow*, Cambridge Univ. Press (Cambridge Texts in Applied Mathematics, 23), Cambridge, 2000.
[3] Chpoun A., Leclerc E., Experimental investigation of the influence of downstream flow conditions on Mach stem height, *Shock Waves* 1999;9:269-71.
[4] Chpoun A., Passerel D., Li H., Ben-Dor G., Reconsideration of oblique shock wave reflection in steady flows, *J..Fluid. Mech*. 1995. Vol.301.P.19-35.
[5] Sebastian Deck, Philippe Duvaeu, Paulo d'Espincy, Philippe Guillen, Development and application of Spalart-Allmaras one equation turbulence model to three dimensional supersonic complex configurations, *Aerospace Science and Technology* pp. 171-183, January 2002.
[6] Marie Claude Druguet, David E. Zeitoun, Influence of numerical and viscous dissipation on shock wave reflections in supersonic steady flows, *Computers and Fluids*, 2003 Vol.32.P.515-533.
[7] Gribben B.J., Badcock K.J., Richards B.E., Numerical study of shock-reflection hysteresis in an underexpanded jet, *AIAA* J.2000 Vol.38.P.275-283.
[8] Ivanov MS, Markelov GN, Kudryavtsev AN, Gimelshein S., Markelov G., Investigation of the hysteresis phenomena in steady shock reflection using kinetic and continuum methods. *Shock Waves* 1996;5:341-6.
[9]G. K.Batchelor, *An Introduction to Fluid Dynamics*, Cambridge Univ. Press, Cambridge, England, 1967.
[10] K.D. Kihm, T.K. Kim, S.Y. Son, Visualization of high speed gas jets and their airblast sprays of cross-injected liquid, *Experiments in Fluids*, 1999 Vol.27.P.102-106.
[11] B.E Launcher and Spalding, The numerical computation of turbulent flows, *Computer Methods in Applied Mechanics and Engineering*, 3:269-289, 1974.

[12] Li H., Ben Dor G., A parametric study of Mach reflection in steady flows, *J. Fluid Mech* 1997;341:101-25.
[13] Patrick H. Oosthuizen, William E. Carscallen, *Compressible fluid flow*, McGraw-Hill, 1997.
[14] P.R. Spalart, S.R. Allmaras, A one equation turbulence model for aerodynamic flows, *AIAA*, 1999.
[15] P.R. Spalart and S.R. Allmaras, A one-equation turbulence model for aerodynamic flows, *Technical Report AIAA-92-0439*, American Institute of Aeronautics and Astronautics, 1992.
[16] Anthony Anderson, Xiaoming Zheng and Vittorio Cristini, Adaptive unstructured volume remeshing, *Journal of Computational Physics, Volume 208, Issue 2, 20 September 2005*
[17 Patankar, S. V. and Spalding, D. B., (1972), A Calculation Procedure for Heat, Mass and Momentum Transfer in Three-dimensional Parabolic Flows. *International Journal for Heat and Mass Transfer*., 15, 1787-1806.
[18] John C.Tannehill,Dale A.Anderson,Richard H.Pletcher, Computational Fluid Mechanics and Heat Transfer, Taylor & Francis Inc, 1997.
[19] N.C. Markatos, Mathematical modelling of single and two phase flow problems in the process industries, Revue de l'Institut Francais du Petrole, Vol.48,No.6, pp 631-632, 1993.
[20] N.C. Markatos, A.C.H. Mace, D.G. Tatchell Analysis of combustion in recirculating flow for rocket exhausts in supersonic streams, J. Spacecraft and Rocket, Vol.19,No.6, pp 557-563, 1982.
[21] N.C. Markatos, On numerical modelling of embedded subsonic flows, Int. J. Num. Methods in Fluids, Vol.6, pp 103-112, 1986.